ILASS 2008
Sep. 8-10, 2008, Como Lake, Italy

Paper ID ILASS08-4-5

EXTENSION AND VALIDATION OF THE CAB DROPLET BREAKUP MODEL TO A WIDE WEBER NUMBER RANGE

Ekaterina Kumzerova*, Thomas Esch°

* New Technologies and Service, Dobrolubova Pr. 14, Saint Petersburg, 197198, Russia,
Katya.Kumzerova@nts-int.spb.ru
° ANSYS Germany, Staudenfeldweg 12, Otterfing, 83624, Germany,
Thomas.Esch@ansys.com

ABSTRACT

The Cascade Atomization and drop Breakup (CAB) model was developed by Tanner [1] for the prediction of high-velocity dense sprays and was initially tuned to "medium" range of Weber numbers (injection Weber numbers $O(10^3)$). In this Weber number regime the model provides good agreement with experiments, but it fails to predict the spray formation at conditions corresponding to relatively "low" (O(10)) or "high" ($O(10^4)$) injection Weber numbers. This study describes a possible extension of the CAB model, so that it can be used for a wider range of Weber numbers.

The modification was implemented into ANSYS CFX and validation was performed for experimental conditions covering a Weber number range from 20 up to 20.000.

Overall the results of the model modification can be summarized as follows: The modified model retains the good properties of the CAB model in the medium Weber number range, while it noticeably improves the CAB model performance at "low" and "high" injection Weber numbers. The improvement covers local droplet size and velocity distributions as well a global spray characteristics, such as tip penetration and spray angle.

INTRODUCTION

The performance of direct injection diesel engines is strongly dependent on the perfection degree of fuel-air mixture in a combustion chamber. The process of mixture generation is mainly affected by the interaction of the fuel spray with the surrounding gas leading to the series of droplet breakups which actually determine the efficiency of fuel evaporation. Detailed modeling of this and other spray processes can lead to significant improvements in performance, quality of product, and reduction of emission of pollutants.

In spite of a lot of numerical studies during last years were devoted to the modeling of fuel atomization behavior the existing of a model describing breakup mechanisms for a wide range of conditions is still a real challenge.

One of the possible approaches to describe secondary droplet breakup is the Cascade Atomization and drop Breakup (CAB) model proposed by Tanner [1]. It is an extension of the well-known Taylor Analogy Breakup (TAB) model, developed by O'Rourke and Amsden [2]. Both models are available in ANSYS CFX [3] and were successfully used for the simulation of non-evaporating and evaporating sprays over a wide range of experimental conditions. In combination with the Blob injection method the CAB model has shown the best results among the secondary breakup models available in ANSYS CFX [4].

The aim of this paper it to describe an extension of the CAB model to a wider range of Weber numbers. The extension was motivated by the following reasons: Originally [1] the CAB model was tuned to "medium" range of Weber numbers (injection Weber numbers $O(10^3)$), where it provides good agreement with experiments. The prediction performance deteriorates for conditions corresponding to relatively "low" (O(10)) or "high" ($O10^4$)) injection Weber numbers.

The proposed modification was implemented into ANSYS CFX and validation was done for several cases corresponding to a wide range of Weber numbers.

NUMERICAL METHOD

All simulations were performed with the latest version of ANSYS CFX [3]. ANSYS CFX is a general purpose, three-dimensional Navier-Stokes code. The Navier-Stokes equations are discretized by an element-based finite volume method in a collocated variable arrangement on unstructured grids. A high resolution discretization scheme is used for the convective terms and a second order backward Euler scheme for the time discretization in order to obtain a second order error reduction in space and time. The mass and momentum equations are solved in an implicit fully coupled manner. For convergence rate enhancement, a multi-grid scheme is incorporated.

The particle tracking module in ANSYS CFX allows tracking representative samples of the actual particles through the flow. Differential equations for the position and velocity of each particle are solved, and the effect of the particles on the fluid is calculated as source terms for the fluid mass, momentum or energy equations, the particle mass can change due to processes such as evaporation or chemical reactions with the fluid. Additional effects on the particle can be modeled by the user, either through the built-in expression language, or by user subroutines.

A wide range of primary and secondary droplet breakup models are available to perform spray type simulations. The post processing of spray simulations is simplified as local and global spray characteristics (droplet size and velocity distributions, tip penetration) are created automatically during runtime.

Special effort has been dedicated to the development of a novel and intelligent load management procedure in order to maintain excellent parallel performance with the particle transport model.

THE STANDARD CAB MODEL

The standard CAB model [1] implies the same droplet deformation mechanism as the TAB model [2], but uses a different relation for the description of the droplet sizes after breakup process. It is assumed that the rate of child droplets generation is proportional to the number of child droplets:

$$\frac{d}{dt}n(t) = 3K_{br}n(t). \qquad (1)$$

The breakup frequency K_{br} depends on the breakup regime (bag, stripping or catastrophic) and is given by:

$$K_{br} = \begin{cases} k_1\omega & 5 < We < We_{t1} \\ k_2\omega\sqrt{We} & We_{t1} < We < We_{t2} \\ k_3\omega We^{3/4} & We_{t2} < We \end{cases}, \qquad (2)$$

where ω is the drop oscillation frequency defined as in the TAB model, We is the Weber number based on the droplet radius.

The bag breakup regime constant $k_1 = 0.05$ was determined to match the experimental data, whereas the values for the constants k_2 and k_3 were chosen to provide continuous K_{br} at the regime-dividing Weber numbers, We_{t1} and We_{t2}.

Assuming a uniform droplet size distribution, the following ratio of child to parent droplet radii can be derived:

$$\frac{r_{p,child}}{r_{p,parent}} = e^{-K_{br}t}. \qquad (3)$$

After breakup of the parent droplet, the deformation parameters of the child droplet are set to $y(0) = \dot{y}(0) = 0$. The child droplets inherit a velocity component normal to the path of the parent droplet with a value of:

$$V_N = A\dot{x}. \qquad (4)$$

A is a constant that is determined from an energy balance consideration [1].

It has been observed that the TAB model often predicts a ratio of child to parent droplet that is too small. This is mainly caused by the assumption, that the initial deformation parameters $y(0)$ and $\dot{y}(0)$ are zero upon injection, which often leads to far too short breakup times. The largely underestimated breakup times in turn lead to an underprediction of global spray parameters such as the penetration depth, as well as of local parameters such as the cross-sectional droplet size distribution. To overcome this limitation Tanner [1, 5] proposed to set the initial value of the rate of droplet deformation to a negative value while still assuming that the initial droplet is undeformed.

The effect of this modification is to delay the first breakup of the large initial droplets and to extend their life span, which results in a more accurate simulation of the jet breakup.

MODEL EXTENSION

It was noticed in [6] that the standard CAB model provides good agreement with the measurements for the medium injection Weber number range ($O(10^3)$) while for very low and for very high Weber numbers large differences were observed.

The proposed model modification is based on the observation that some of the model constants show a dependence on the injection Weber number. This can be seen very clearly in Fig.1 that shows the spray tip penetration for a high pressure diesel injection case [7]. In this experiment, diesel fuel at high pressure (1600 bar) was injected through a nozzle with 0.167 mm diameter into stagnant gas with a pressure of 50 bars and a temperature equal to 710 K. The resulting injection Weber number is about 20.000. From the figure it can be seen that a variation of k_1 has a significant impact on the penetration of the liquid phase.

The idea of the modification is based on the assumption that the bag breakup factor, k_1, is a function of the injection Weber number. Such a correlation was obtained on the basis of several cases corresponding to significantly different values of the injection Weber number. For each of the selected test cases both global (spray penetration depth and spray angle) and local (droplet size and velocity distributions) characteristics were known from the experiment.

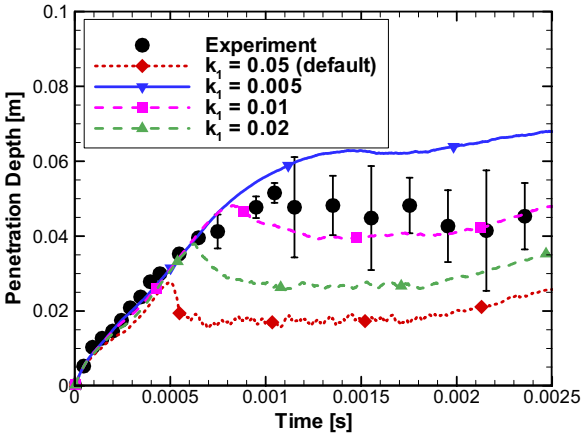

Fig 1. Influence of the CAB model breakup coefficient k_1 on the spray tip penetration for high pressure injection [7].

The following correlation is proposed for the modification of the bag breakup coefficient:

$$k_1(We_0) = \begin{cases} k_1^{low}, & We_0 < We^{\min} \\ k_{factor} \cdot We_0^{k_{power}}, & We^{\min} < We_0 < We^{\max} \\ k_1^{high}, & We_0 > We^{\max} \end{cases} \qquad (5)$$

with

$$We_0 = \max(We_{inj}, We_{cur}). \qquad (6)$$

For injection Weber numbers below a lower limit We^{min} or above an upper limit We^{max} the bag breakup coefficient is assumed to be constant in order to avoid unphysical values for this parameter.

Between the upper and lower Weber number limits the calculation of k_1 is based on the largest Weber along the particle trajectory. This is typically the injection Weber

number, We_{inj}. For cases where the local particle Weber exceeds the injection Weber number (for example droplets in free jet), this Weber number is used.

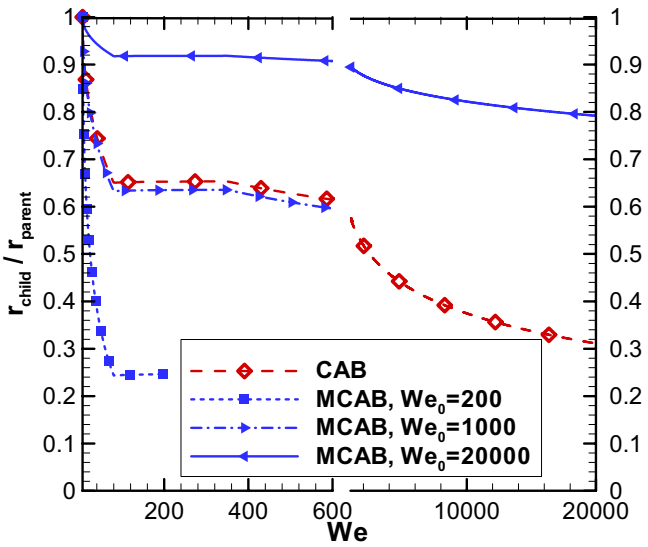

Fig 2. Ratio of the injection mean product/parent drop radii in dependence on the Weber number for inviscid liquid.

The ratio of the product/parent droplet radius computed with k_1=*0.05* for the standard CAB model and using Eq. (5) for the modified CAB model is presented in Fig. 2. For the modified CAB model as suggested this ratio depends on the injection (or maximum) Weber number. At that the initial radii ratio is increased with increasing initial Weber number.

Both models show similar results for intermediate initial Weber numbers (see the dash-dotted curve corresponding to We_0= 1000) while for the large and small initial Weber numbers the ratio of the product/parent drop radii is significantly different.

CASE DESCRIPTION AND SET-UP

To tune the constants k_1^{low}, k_{factor}, k_{power} and k_1^{high}, five different cases were run covering a wide range of injection Weber numbers.

The initial test cases simulated the experiments of Liu and Reitz [8] where droplets with a constant diameter of 170 µm were injected into a vertical jet of air under normal atmospheric conditions (1 bar) with a horizontal velocity of 16 m/s. The velocity of the vertical jet was varied between 0 and 100 m/s. The resulting initial Weber numbers varied between 30 and 100 (see Table 1). From the experiment droplet sizes after breakup and droplet trajectories were known for the comparison between the experiment [8] and the numerical simulation.

For all computations the k-epsilon turbulence model was used. The coupling between the phases was modelled via the Schiller-Naumann drag correlation.

These simulations were run as a steady state. In a first step, the Euler flow field was solved until the normalized maximum residuals of the momentum equations were below a value of 10^{-6}. Starting from this solution only one time step was done with one-way coupled particles to obtain particles trajectories. To provide grid-independent solution the numerical mesh corresponded to a cylinder with 200.000 nodes with finer resolution inside the o-block and in the axial direction close to the injector was used.

Table 1. Data for the experiment of Liu and Reitz [8].

Case Name	Air Velocity (m/s)	Maximum Weber Number
Case 2	59	18
Case 3	72	26
Case 4	100	51

Next, non-evaporating and evaporating sprays were investigated. Table 2 compiles the spray and gas parameters of the four different experimental setups for the solid-cone injections.

Table 2. Data for single-hole solid cone injections.

Case Reference	Hiroyasu & Kadota [9]	Schneider [10]	Bosch	Deutz [7]
Gas Parameters				
Gas Type	N_2	N_2	Air	Air
Temperature (K)	300	395	300	710
Pressure (MPa)	1.1, 3.0, 5.0	1.5	0.11, 0.56	5
Fuel Properties				
Fuel type	$C_{12}H_{26}$	$C_{12}H_{26}$	nHeptane	Diesel
Density (kg/m^3)	840	840	640	810
Surface tension (N/m)	0.0205	0.0205	0.02	0.016
Spray Parameters				
Temperature (K)	300	300	293	303
Maximal injection velocity (m/s)	102, 90, 86	183	138	456
Maximal particle mass flow rate (g/s)	6.05, 5.36, 5.13	2.7	1.5	6.8
Nozzle diameter (mm)	0.3	0.15	0.151	0.167
Injection rate, single pulse (ms)	2.5, 4.0, 4.0	1.2	1.5	2.25
Initial spray angle (deg)	7.5, 12.4, 16	7.5	2.6, 6	8.4
Injection Weber number	900, 2000, 3050	2050	85, 450	20000

These cases were run as unsteady. As the sprays were assumed to be axis-symmetric the computational domain corresponded to a 6 degree cylinder section with finer resolution on the centerline and close to the injector. The simulations were done on the grid with 9700 nodes which was sufficient for grid-independent solutions.

The flow was assumed to have converged within a transient time step when the maximum residuals fell below a tolerance of 0.001.

For the comparison between the numerical simulations and the experiments global spray characteristics, such as the tip penetration or the spray angle were used. Whenever possible also local spray properties, such as the drop trajectories or size distributions were compared with the measurements.

RESULTS AND DISCUSSION

Single droplet in cross flow

From the experiment [8] the trajectory measurements are known for cases 2 and 4 and droplet size data are known for cases 2 and 3. In Fig. 3 the computed and experimental drop trajectories for case 2 are presented. The next figure (see Fig. 4) shows the comparison between the numerically predicted and the measured Sauter mean droplet diameter for the same case. It can be seen that the standard CAB model slightly overpredicts the droplet diameter after breakup which in turn results in an overprediction of the droplet penetration into the free jet. The modified CAB model improves the agreement in droplet sizes and as a result the computed trajectory also has a better agreement with the measurements.

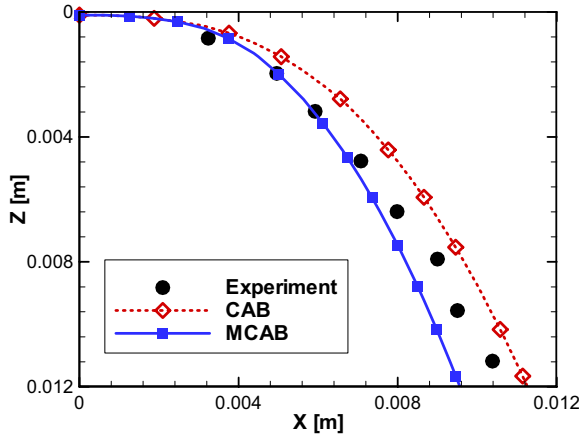

Fig 3. Comparison of droplet trajectories, Case 2 Liu and Reitz [8].

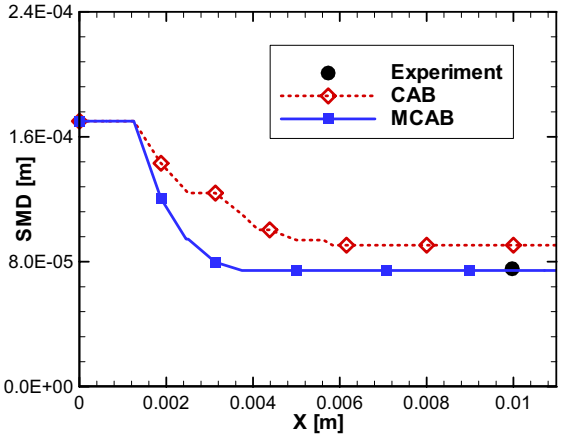

Fig 4. Comparison of droplet Sauter mean diameters, Case 2, Liu and Reitz [8].

As similar results can be seen for case 3 (see Fig. 5). Here again the predicted droplet sizes are closer to the experimental data relative to the standard model.

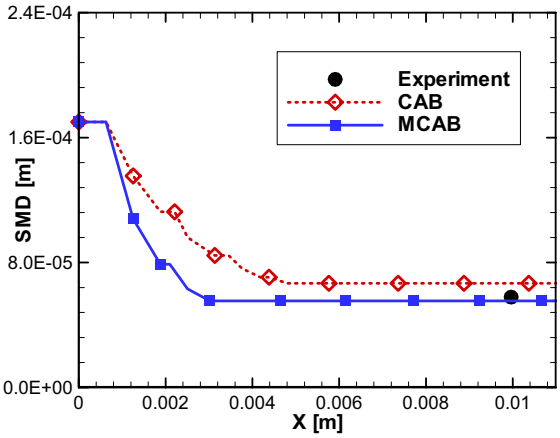

Fig 5. Comparison of droplet Sauter mean diameters, Case 3, Liu and Reitz [8].

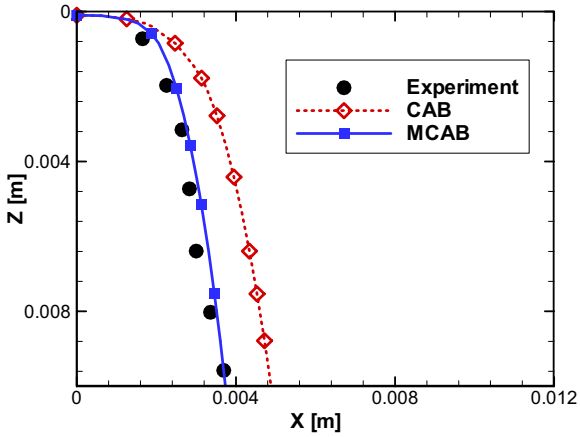

Fig 6. Comparison of droplet trajectories, Case 4, Liu and Reitz [8].

The agreement for case 4 presented in Fig. 6 is also significantly better than with the standard CAB model

The Weber numbers for all the presented cases are well below the lower Weber number limit, We^{min}, which means that the resulting breakup factor is constant and equal to k_1^{low}.

Single-hole solid-cone injections

This section presents results for single-hole injections ranging from low (85, Bosch 1) to high (20.000, DEUTZ) injection Weber numbers.

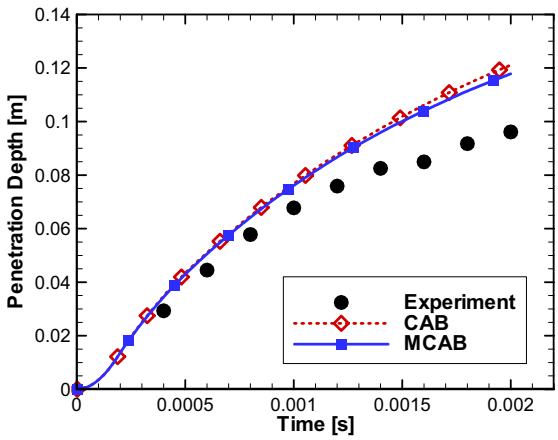

Fig 7. Spray tip penetration versus time, Bosch case 1.

Fig. 7 and 8 show global and local spray data for the low Weber number Bosch case 1. Local data are presented at the position 30 mm from the injector nozzle exit. It can be seen that the suggested model modification slightly improves the spray tip penetration as well as the droplet diameter and velocity distributions.

The standard CAB model overpredicts the droplet sizes and also the droplet velocities which results in a larger spray penetration. The modified model predicts smaller mean droplet sizes after breakup which in turn also improves the droplet velocity distribution.

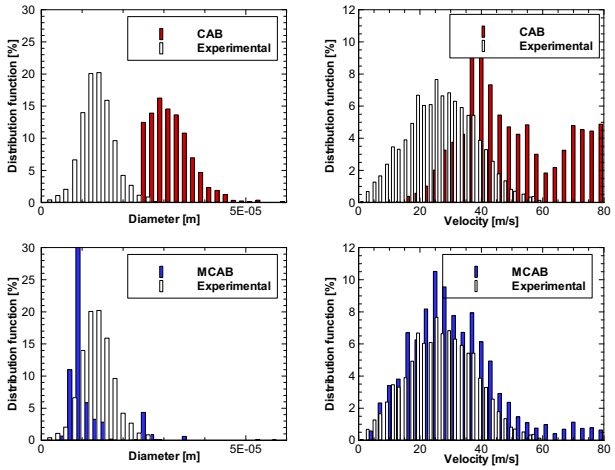

Fig 8. Comparison of droplet size (left) and velocity (right) distributions for Bosch case 1. Top: Standard CAB, Bottom: Modified CAB.

The results for Bosch case 2 that correspond to a larger injection Weber number are presented in Fig 9 and 10. The standard model has already shown good agreement for both global and local spray characteristics. It can be seen that the modified model preserves this agreement for the tip penetration. The mean droplet size predicted by the modified model is a little bit smaller than for the standard CAB model but it still agrees well with measurements. A slight improvement for the velocity distributions could also be achieved.

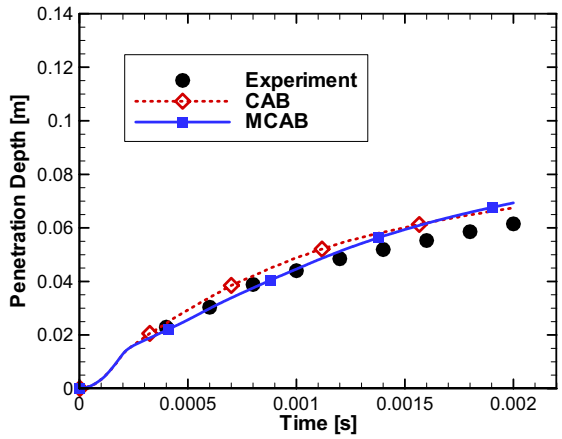

Fig 9. Spray tip penetration versus time, Bosch case 2.

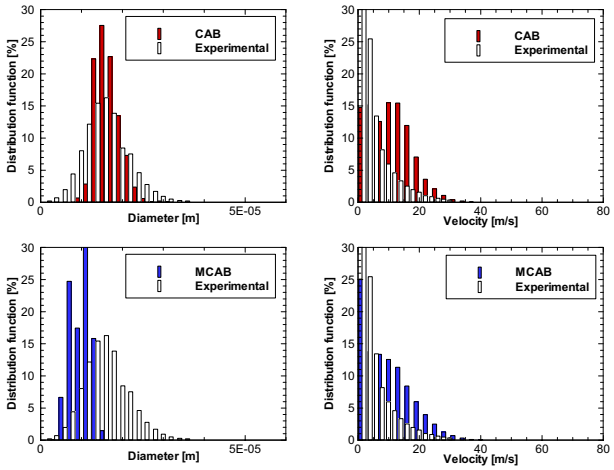

Fig 10. Comparison of droplet size (left) and velocity (right) distributions for Bosch case 2. Top: Standard CAB, Bottom: Modified CAB.

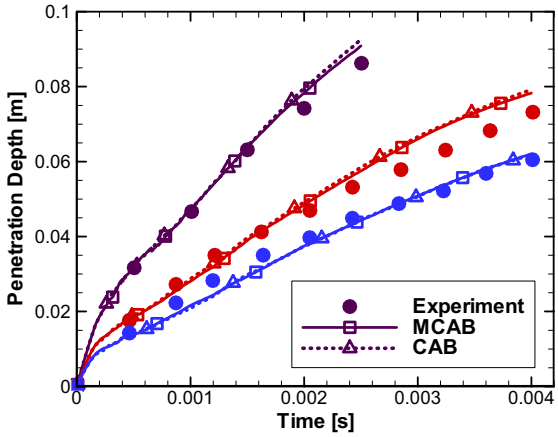

Fig 11. Spray tip penetration versus time, Hiroyasu and Kadota [9], cases 1-3.

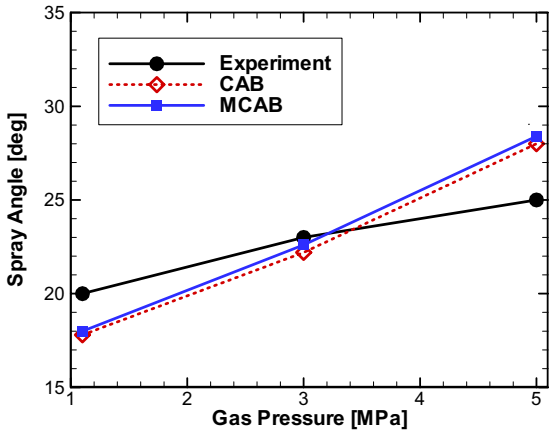

Fig 12. Spray angles versus gas pressure in a chamber, Hiroyasu and Kadota [9].

The next figures (Fig. 11 and 12) show results for the cases of Hiroyasu & Kadota [9]. These cases correspond to a medium injection Weber number range where the standard CAB model has already been successfully used for the prediction of the spray injection. As desired there is no negative impact on the application of the model modification. In particular, Figure 11 shows that the experimental tip penetration for all chamber pressure levels agrees very well with computations using both the CAB and the modified model. A small impact can be seen for the spray angles (see

Fig. 12). Slight disagreement between the experimental data and the computations can be explained by non-matching definitions of the spray angle both in simulations and measurements.

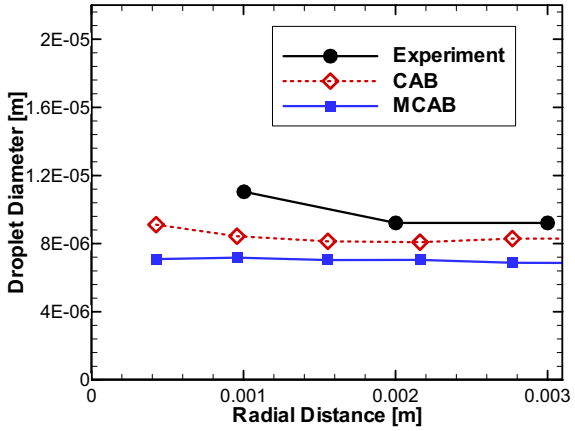

Fig 13. Mean droplet radii distributions along spray cross-section, Schneider [10].

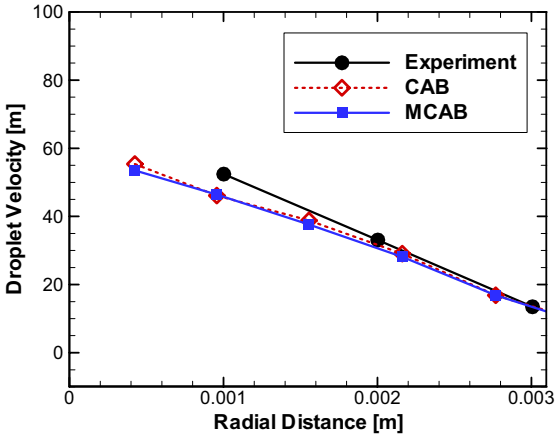

Fig 14. Mean axial velocity distributions along spray cross-section, Schneider [10].

In the Fig. 13 and 14 the radial distributions of the mean droplet size and velocity at a nozzle distance of 25 mm are presented and compared to the measurements of Schneider [10]. Small underestimation compared to the standard CAB model can be observed for the droplet radii distributions (see Fig. 13). At the same time the velocity distribution (see Fig. 14) did not change so the overall agreement with the experiments for the modified model can be said to be the same as for the standard CAB model.

The last case presented here is a high pressure diesel injection case with droplet evaporation. The injection Weber number for this case is approximately 20.000. Significant improvements can be seen by applying the suggested model modification as compared to the standard CAB model. Fig. 15 shows that the droplet sizes are strongly underestimated by the standard CAB model which results in an underprediction of the liquid penetration depth. This effect is further enhanced by the fact that droplet evaporation is strongly influenced by the current droplet size. The suggested modification significantly increases droplet sizes after breakup which leads to lower evaporation rates and correspondingly to a larger liquid penetration.

From the experiment the droplet size and velocity distributions are known at 40 mm downstream of the nozzle exit. As can be seen in Fig. 15 the maximum penetration computed with the CAB model is less than 30 mm which means that at the position of 40 mm there are no droplets and no comparison for the size and the velocity distributions can be made. The comparisons for the modified CAB model are presented in Fig. 16. It can be seen that the prediction of both the droplet size distribution and the droplet velocity distribution agrees very well with the measurements.

The decrease of the liquid penetration 2.4 ms after begin of the injection is caused by the fact that the mass flow rate is decreased. This leads to a decrease of the injection Weber number which in turn increases the value of the constant k_1.

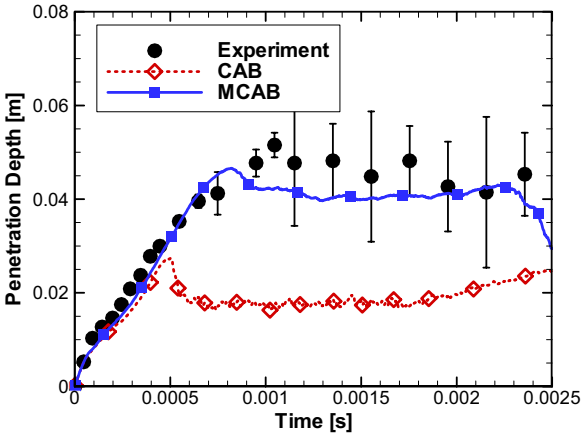

Fig 15. Comparison of the spray tip penetration versus time, DEUTZ case [7].

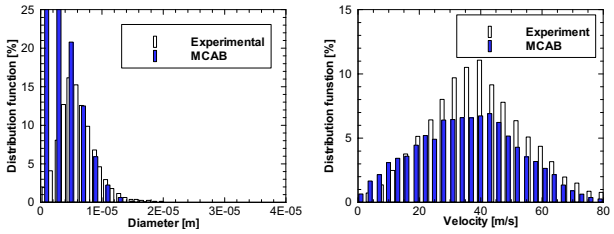

Fig 16. Comparison of droplet size (left) and velocity (right) distributions for the DEUTZ case [7]. Modified CAB model.

CONCLUSIONS

An extension of CAB droplet breakup model to a wide Weber number range was proposed. Validation of this model was carried out for five cases corresponding to significantly different Weber numbers.

Results of the implemented modification can be summarized as following:

- The modified model retains the good properties of the CAB model in the medium Weber number range, while it significantly improves the CAB model performance at “low” and “high” injection Weber numbers.
- Improvements for the “low” Weber number were obtained for the droplet trajectories in free jets as well as for the droplet size and velocity distributions for solid-cone injections.
- Significant improvement was achieved for evaporating sprays with “high” initial Weber numbers for local and global spray characteristics.

The results that were obtained so far are very encouraging. Further validation studies for the application of the modified CAB model in internal combustion engines will be carried out in the near future.

NOMENCLATURE

Symbol	Quantity	SI Unit
CAB	Cascade Atomization and Drop Breakup	
MCAB	Modified CAB	
SMD	Sauter Mean Diameter	
TAB	Taylor Analogy Breakup	
A	Radial product drop velocity coefficient	
K_{br}	Breakup Frequency	s^{-1}
We	Weber number based on droplet radius	
We_0	Initial Weber number	
We_{t1}	Critical Weber number of stripping breakup, = 80	
We_{t2}	Critical Weber number of catastrophic breakup, = 350	
We_{min}	Constant, = 55	
We_{max}	Constant, 10000	
k_1	CAB model bag breakup coefficient	
k_1^{low}	MCAB model breakup coefficient, = 0.1	
k_1^{high}	MCAB model breakup coefficient, = 0.01	
k_{factor}	MCAB model breakup coefficient, = 6.7	
k_{power}	MCAB model breakup coefficient, = -0.7	
n	Number of the product droplets	
r	Droplet radius	m
t	time	s
v_n	Normal velocity	$m\ s^{-1}$
x	Droplet deformation	m
y	Normalized drop deformation (=$x/2r$)	
Ω	Drop oscillation frequency	s^{-1}

Subscripts

child	Child
cur	Current
inj	Injection
parent	Parent

REFERENCES

[1] F. X. Tanner, Development and validation of a cascade atomization and drop breakup model for high-velocity dense sprays, *Atomization and Sprays*, vol. 14, number 3, pp. 1-32, 2004.

[2] P.J.O'Rourke and A.A. Amsden, The TAB Method for Numerical Calculation of Spray Droplet Breakup, *SAE Technical Paper*, 872089, 1987.

[3] ANSYS, CFX 11 Documentation, 2007.

[4] E. Kumzerova, T. Esch and F. Menter, Spray simulations: application of various droplet break-up models, *Proc. 6th International Conference on Multiphase Flow 2007*, No. S4_Tue_D_27, 10p, 2007.

[5] F.X. Tanner. Liquid Jet Atomization and Droplet Breakup Modeling of Non-Evaporating Diesel Fuel Sprays, *SAE Technical Paper Series*, 970050, 1997.

[6] E. Kumzerova and T. Esch, Validation of Spray Simulations in ANSYS CFX, *ANSYS CFX Validation Report*, 98 p, 2008.

[7] W. Waidman, A. Boemer and M. Braun, Adjustment and verification of model parameters for Diesel injection CFD simulation, *SAE Technical Paper,* 2006-01-0241, 11 p, 2006.

[8] A.B. Liu and R.D Reitz, Mechanisms of Air-Assisted Liquid Atomization. *Atomization and Sprays*, Vol.3, pp. 1-21, 1992.

[9] H. Hiroyasu and T. Kadota, Fuel Droplet Size Distribution in Diesel Combustion Chamber, *SAE Technical Paper,* 740715, 1974.

[10] Schneider, B. Experimental Investigation of Diesel Sprays, *CRFD and Laser Diagnostic Workshop, 21st CIMAC Congress 1995, Interlaken*, 1995.